

Exploring commercial GNSS RO products for Planetary Boundary Layer studies in the Arctic Region

Manisha Ganeshan^{1,2}, Dong L. Wu¹, Joseph Santanello³, Jie Gong¹, Chi Ao⁴, Panagiotis Vergados⁴ and Kevin Nelson⁴

5 ¹Climate and Radiation Laboratory, NASA Goddard Space Flight Center, Greenbelt, 20771, USA

²Morgan State University, Baltimore, 21251, USA

³Hydrological Sciences Laboratory, NASA Goddard Space Flight Center, Greenbelt, 20771, USA

⁴NASA Jet Propulsion Laboratory, California Institute of Technology, Pasadena, 91109, USA

10 *Correspondence to:* Manisha Ganeshan (manisha.ganeshan@nasa.gov)

Abstract.

Commercial Radio Occultation (RO) satellites that track radio signals from the Global Navigation Satellite System (GNSS) are being touted for their observations in polar regions where RO missions such as COSMIC-2 lack orbital coverage. This study seeks to explore the value of commercial RO satellites, viz. Spire and GeoOptics, for planetary boundary layer (PBL) investigations in the Arctic, a region where favourable lower atmospheric penetration of GNSS RO is vital for representing the persistently shallow PBL. Both Spire and GeoOptics have seemingly improved lower tropospheric penetration capability over the Arctic Ocean compared to other RO missions such as MetOp, with Spire having nearly one order (two orders) of magnitude greater volume of observations at 500 meters above mean sea level compared to MetOp (GeoOptics). The RO-derived monthly mean Arctic PBL height (PBLH) from GeoOptics is comparable to that retrieved from MetOp as well as the PBLH in the Modern-Era Retrospective analysis for Research and Applications version 2 (MERRA-2). The PBLH retrieved from NASA-purchased Spire data has relatively less spatial and seasonal variability compared to other datasets. A cut-off altitude threshold of 500 meters for minimum RO penetration height works sufficiently well for representing the Arctic PBLH in all datasets except for NASA-purchased Spire data which performs better when 300 meters threshold is used. Arctic PBLH representation is not strongly affected by the total number of available observations, the minimum RO penetration altitude, or instrument type, but instead appears to be sensitive to the choice of processing algorithm used for retrieving bending angle and refractivity profiles. This is the key factor which influences the rate of penetration loss in the lower troposphere as well as the PBLH representation.

1 Introduction

The planetary boundary layer (PBL) is a target observable of broad importance to the Earth Science community. The Global Navigation Satellite System (GNSS) Radio Occultation (RO) has been shown to be a good candidate for observing the PBL height (PBLH) across various spatiotemporal scales (Ao et al., 2012; Basha and Ratnam, 2009; Ding et al., 2021; Kalmus et

al., 2022; Nelson et al., 2021; Winning et al., 2017) as recommended by the National Academies of Science Decadal Survey for Earth Science and Applications from Space report (NASEM, 2018; Teixeira et al., 2021). Today, advancing PBL science is inherently reliant on high resolution observations with high-frequency sampling that can chiefly be afforded by a single
35 remote sensing instrument/combination of instruments from space. In this regard, GNSS RO is a vital measurement technique, due to its superior vertical resolution (< 100 m) and viewing geometry compared to most other nadir-viewing space-based instrument technologies, allowing penetration down to 100 meters above surface. High vertical resolution measurements and deep penetration of observations into the lower atmosphere are deemed vital for polar regions, where it is particularly difficult to observe and characterize the persistent surface-based PBL temperature inversions.

40

1.1 Importance of GNSS RO for Arctic PBL studies: Why commercial data?

The study of the Arctic Ocean PBL can greatly benefit from GNSS RO observations, which offer: (a) continuous sampling under all weather conditions, (b) the ability to observe beneath the persistent stratus cloud cover, (c) improved performance over flat surfaces (sea ice, open ocean) compared to sharp varying slopes (land mass), and (d) a long-term data record spanning
45 more than two decades with added coverage from recently launched commercial satellites. Commercial satellites are particularly advantageous for high-latitude polar studies where there is a notable lapse in coverage following the decommissioning of the Constellation Observing System for Meteorology Ionosphere and Climate (COSMIC-1) in 2019. The follow-on mission to COSMIC-1, COSMIC-2, only covers 45°N to 45°S . It is expected that coverage from private sector GNSS RO satellites fills the gaps in the climate data record. First, however, it is necessary to explore the lower atmospheric
50 sounding capability of these commercial missions in comparison to past and current existing operational GNSS RO products in the Arctic, where the gradient method used for determining the PBL height (Ao et al., 2012; Nelson et al., 2021; Qiu et al., 2023; Seidel et al., 2010, 2012) is found to be sensitive to the penetration capability of RO profiles (Ganeshan and Wu, 2015). From the analysis of 8 years of COSMIC-1 data, it was found that availability of RO profiles over the Arctic Ocean reduced significantly at tangent heights below 1km, which introduces a sensitivity of the retrieved PBL height to the choice of the cut-
55 off altitude, or minimum RO penetration depth, used for profile selection. However, it was noted that only the absolute PBLH values were sensitive to the choice of cut-off altitude, whereas the spatial and seasonal variability remained largely unaffected (Ganeshan and Wu, 2015). Regardless, it is worthwhile to compare the lower atmospheric penetration capability among various GNSS RO products and to explore factors that can influence this capability, and in turn, influence the observation of the Arctic PBLH.

60

1.2 A background of GNSS RO neutral atmosphere technique

In the GNSS RO technique, the neutral atmosphere is considered as the atmospheric path consisting of the troposphere and stratosphere (up to 60 km) which is refractive and electrically neutral, unlike the mesosphere and ionosphere-thermosphere regions. The neutral atmosphere has both dry and wet components that contribute to the refraction, with the wet component
65 becoming more important closer to the surface due to increased concentrations of water vapor. Not all RO profiles reach the

surface, and in fact, there can be an exponential drop in the fraction of available RO observations (penetration probability) as we go towards the surface (Ganeshan and Wu, 2015) which is primarily due to the decrease in the signal-to-noise ratio (SNR) caused by atmospheric defocusing (Wu et al., 2022). However, factors such as instrument design, neutral atmosphere excess phase computation method, and choice of bending angle retrieval algorithm can also affect the penetration probability profile
70 for a given atmospheric path.

A thorough understanding of factors affecting RO penetration is desirable to help minimize sampling bias as well as to ensure data continuity and consistency in climate records. However, this is difficult to achieve, given the existence of a large number of GNSS RO missions and different versions of products from a single mission that are periodically reprocessed to remain up
75 to date with advances in software and processing algorithms. This study aims to provide a comparison of the penetration capability of new commercial GNSS RO data products against other existing products in the Arctic as the first step towards establishing a climate ready, long-term continuous, dataset that can be used for Arctic PBL investigations.

2 Data and Methodology

2.1 GNSS RO

80 2.1.1. Commercial RO Datasets

The goal of this study is to explore the value of commercial GNSS RO products for PBL studies in the Arctic Ocean (north of 60°N excluding land areas) by comparing with other GNSS RO mission products such as, COSMIC-1 and the Meteorological Operational satellite programme (MetOp). The commercial GNSS RO data evaluated in this study are purchased by NASA through the Commercial SmallSat Data Acquisition (CSDA) program. In addition, this study also compares freely available
85 commercial data purchased for near-real time operations by NOAA, for available periods of overlap with the NASA- purchased commercial data.

NASA-purchased Spire data are available from November 2019 through January 2022, and NASA-purchased GeoOptics data are available from January 2020 to April 2021. Spire data are provided at a similar vertical grid and resolution as other GNSS
90 RO missions (such as COSMIC, COSMIC-2, and MetOp) where the lowest level of valid observations differs from profile to profile, because the penetration depth achieved by each RO is unique, depending primarily on the SNR. GeoOptics data, on the other hand, are provided on a uniform 100 m vertical grid, along with a quality flag that is used to determine the lowest penetration level. GeoOptics uses the phase matching methodology in RO processing (Jensen et al., 2004), a wave optics technique designed to extract the full information from the received wave field. The quality flag is applied in two ways: (i)
95 blanket criteria that checks the range of the amplitude of computed phase matching integral and cumulative number of phase jumps within the upper neutral atmosphere (between 8 to 40 km), cutting off the profile at lower levels if the above checks are failed, and (ii) individual criteria that flag each level as “good” or “bad” based on the presence or absence of sharp features

(moisture and temperature gradients) that can cause significant deviation of the bending angle relative to a smoothed background bending angle profile. In this study, only profiles satisfying the blanket criteria are considered as the focus is on the lower troposphere (surface to 5 km). Moreover, each of these profiles are evaluated individually to determine the minimum penetration depth ascertained by the lowest above-surface level with a “good” quality flag. It is important to note that if a “sharp” PBL inversion layer with poor quality control (QC) flag exists above the minimum penetration depth, that profile is not discarded.

The NOAA Spire and GeoOptics data purchased for near-real time operations are downloaded from the University Corporation for Atmospheric Research (UCAR; <http://www.cosmic.ucar.edu/>) website. In the case of GeoOptics, the overlap between NOAA and NASA data is during the month of April 2021, and for Spire, the month of October 2021 is chosen to compare overlapping data. All references to “Spire” and “GeoOptics” in this paper imply NASA purchased commercial RO data unless explicitly specified to be NOAA-purchased datasets.

110

2.1.2. Other datasets

A major focus of this study will be the comparisons between three contemporaneous datasets, viz. NASA Spire, NASA GeoOptics, and the re-processed EUMETSAT MetOp data from the Radio Occultation Meteorology Satellite Applications Facility (ROM SAF). In addition, COSMIC-1 and COSMIC-2 data from the University Corporation for Atmospheric Research (UCAR) will be used to compare RO penetration statistics. Two versions of UCAR reprocessed COSMIC-1 data (2013.3520 and 2021.0390) are obtained for the period ranging from 2007 to 2013 and from 2007 to 2017, respectively. COSMIC-1 data ceased to be produced beyond 2019, thereby limiting their use for this comparative analysis which is focused on the year 2020. For this study, they serve as a climatological record of RO penetration statistics over the Arctic Ocean against which characteristics of newer datasets can be compared. To remove ambiguity resulting from software updates - and to ensure consistency - only those RO mission products that have been re-processed with the same software version are compared against Spire and GeoOptics.

120

2.1.3. Deriving PBLH from GNSS RO

The PBLH is derived from the GNSS RO refractivity profile using the bottom-up search approach described in Ganeshan and Wu (2015), identifying the first minima of the refractivity gradient to exceed -40 N-unit km^{-1} and assigning the corresponding altitude as the PBLH. This approach is specifically useful for deriving the height of the PBL inversion over the Arctic during winter months. A cut-off altitude threshold (which is a required penetration threshold), set to 500 m, is applied to only include RO profiles that reach this altitude or lower. This is the typical cut-off altitude used for GNSS RO based PBL studies (Ao et al., 2012, Guo et al., 2011) that has also proven useful for Arctic PBLH retrieval (Ganeshan and Wu, 2015). Ganeshan and Wu (2015) showed that even though the magnitude of the retrieved PBLH is sensitive to the cut-off altitude, its spatiotemporal variability remained unaffected by the choice of this threshold. All GNSS RO derived monthly mean penetration probability

130

and monthly PBL height characteristics are interpolated onto a 2° latitude x 10° longitude grid, as in Ganeshan and Wu (2015). A distance-weighted averaging method is used for interpolation by considering observations falling within a circle of 5° around each grid point. A nine-point local smoothing is further performed on PBLH values derived from GeoOptics and MetOp observations to help minimize random variations due to smaller sample size.

2.2 Reanalysis Data

The MERRA-2 reanalysis product (Gelaro et al., 2017) is used to obtain the monthly mean PBL height and the monthly mean sea ice fraction over the Arctic Ocean. In MERRA-2, the PBL depth is defined as the model level where the eddy heat diffusivity coefficient (K_H) value falls below $2 \text{ m}^2 \text{ s}^{-1}$ threshold (McGrath-Spangler et al., 2015). The GEOS atmospheric model used in MERRA-2 includes separate parameterizations for stable and unstable PBLs. The non-local Lock et al. (2000) scheme is used to parameterize turbulence in unstable boundary layers, whereas, the model employs a first-order local turbulence closure scheme, Louis et al. (1982), for stable boundary layers. The Louis scheme is expected to be more active in regions such as the Arctic Ocean which are typically characterized by stable conditions. The scheme estimates heat and momentum diffusivity coefficients based on the turbulent length scale and bulk Richardson number at each time step wherein the former is determined by the PBL depth from the previous time step (Ganeshan and Yang, 2019). In case of persistent stable conditions, such as over the frozen Arctic Ocean, the turbulent length scales are expectedly small, implying that the model diffusivity coefficients are largely based on the bulk Richardson number. Thus, MERRA-2 PBLH over Arctic is inherently sensitive to wind and temperature gradients (used for computing the bulk Richardson number), making it comparable to the PBL temperature inversion which is detected by GNSS RO.

In general, the first model level over the Arctic Ocean is around 50 meters above surface and the vertical grid spacing is approximately 100 meters within the lowest five model levels. The horizontal resolution of MERRA-2 products is approximately ~ 0.5 degrees. The MERRA-2 variables are similarly interpolated onto the $2^\circ \times 10^\circ$ horizontal grid (described in section 2.1.3), for ease of comparison. The MERRA-2 vertical grid is based on a terrain-following sigma coordinate system.

155 3 Results and Discussion

3.1 Sensitivity of RO penetration loss to bending angle retrieval method

GNSS RO bending angle and refractivity profile observations are characterized by a loss of signal (decrease in SNR) as they approach the surface due to atmospheric defocusing (Wu et al., 2022). However, the rate of penetration loss is expectedly different for various RO missions, due to diversity in the design of GNSS receivers and SNR capabilities. Penetration loss can also be different for measurements from the same instrument, due to inherent disparity in excess phase computations and bending angle retrieval algorithms. For example, older versions of the same product, such as the UCAR COSMIC-1 2013.3520 version, can differ significantly from newer reprocessed versions (e.g., COSMIC-1 2021.0390), due to advances in excess phase computations, retrieval software, GNSS orbits, clock, and earth orientation products (UCAR Data Release, 2022).

Figure 1 compares the rate of RO penetration loss over the Arctic Ocean for different GNSS RO missions (COSMIC, MetOp, Spire, GeoOptics) as well as for different products from the same mission (e.g., COSMIC-1 2013.3520 vs. COSMIC-1 2021.0390; Spire NASA vs. Spire NOAA; GeoOptics NASA vs. GeoOptics NOAA). Clearly, the penetration loss is less significant for the newer version of COSMIC-1 data compared to the older version, due to major advances in computations and retrieval software. For contemporaneously processed commercial data products, viz. Spire NASA vs Spire NOAA and/or GeoOptics NASA vs. GeoOptics NOAA, the differences in penetration probability are generally confined to the lowest 1 km. These differences are solely due to the choice of processing algorithm used for retrieving the bending angle and refractivity profiles. The Spire NOAA data are similar to the reprocessed COSMIC-1 2021.0390 data, despite differences in SNR between the two products, with more than 50% of the profiles penetrating down to 200 m above the surface, as opposed to less than 5% for MetOp and Spire NASA data.

Figure 2 (a) shows the RO penetration probability for a common subset of NASA-purchased and NOAA-purchased Spire profiles. The former is processed by the vendor, while the latter is processed by UCAR from the L1b purchased data. Even though the same physical ROs are compared, the two products show distinctive penetration patterns below 500 meters. On the contrary, when comparing NOAA Spire profiles with COSMIC-2 profiles over the tropics, both processed by UCAR, there is little to no difference in the penetration probabilities (Fig. 2(b)). Thus, processing software appears to have a greater bearing on RO penetration loss compared to instrument hardware.

180

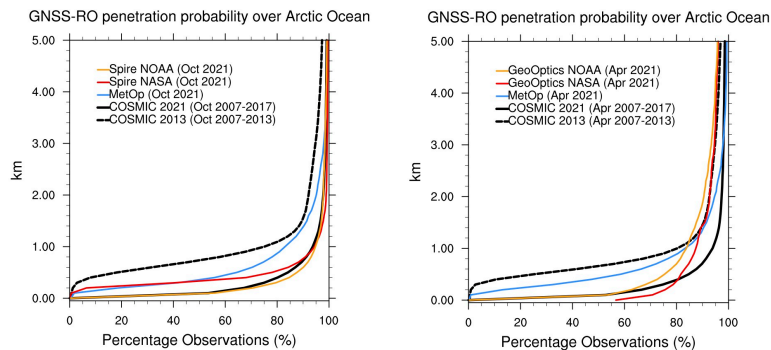
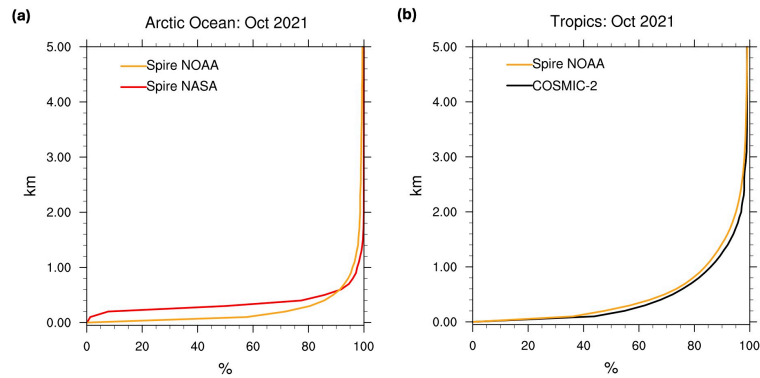


Fig. 1 RO penetration loss as a function of altitude over the Arctic Ocean (north of 60°N) from different products comparing **(left)** COSMIC-1, MetOp, and Spire for the month of October and **(right)** COSMIC-1, MetOp, and GeoOptics for the month of April.



185

Fig. 2 RO penetration loss as a function of altitude for October 2021 showing (a) differences in penetration probabilities for a common subset of monthly ROs over the Arctic Ocean obtained from a single mission/instrument (Spire) processed by different centers and (b) similarities in penetration probabilities for different sources of monthly ROs over the Tropics (30°S to 30°N) obtained from two separate missions but processed by the same center (UCAR).

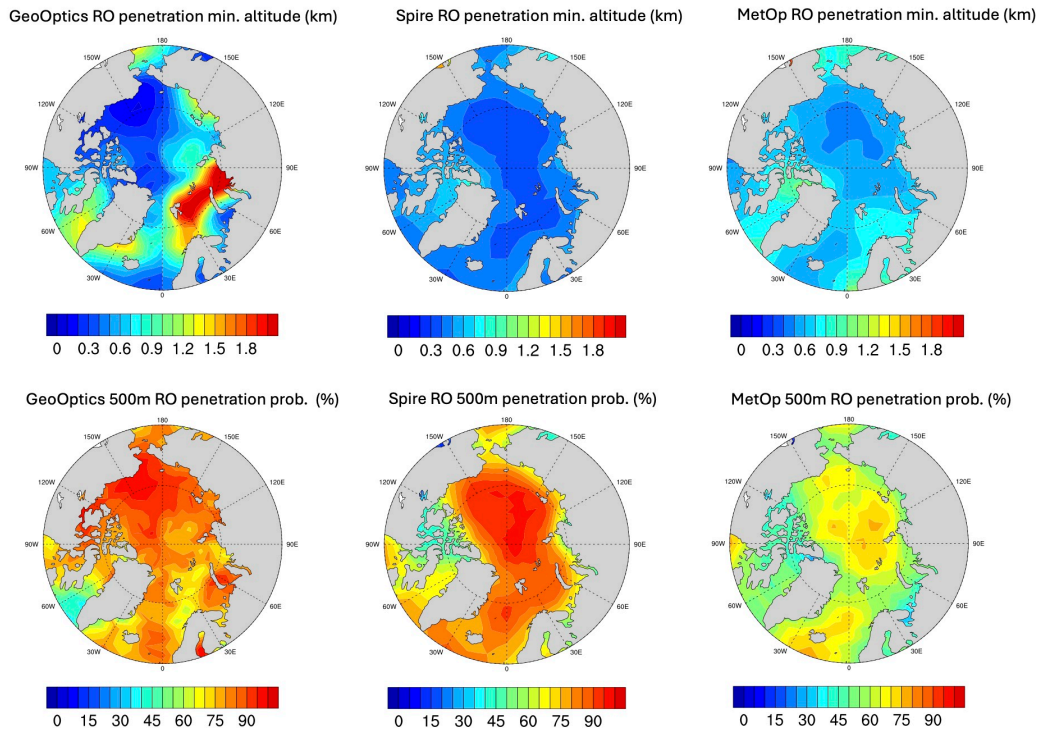
190

3.2 RO penetration over the Arctic Ocean

The top row of Figure 3 compares the minimum altitude of RO penetration over the Arctic Ocean for NASA Spire, NASA GeoOptics, and MetOp data. Spire has deeper penetration throughout the Arctic Ocean compared to MetOp, which is expected, due to the less pronounced rate of loss of penetration below 3 km (as seen in Fig. 1). GeoOptics has the lowest and highest values of minimum RO penetration altitude compared to the other two datasets, with the lows occurring over the frozen ocean in the Beaufort Sea region and to the north of Greenland, and the highs occurring over the Atlantic storm track region. A similar pattern of enhanced RO penetration loss in the storm track region was also observed in COSMIC-1 data (Ganeshan and Wu, 2015). The minimum penetration capability of MetOp is higher over the frozen Arctic Ocean compared to the open ice-free ocean, a pattern that was similarly observed for COSMIC-1 data (Ganeshan and Wu, 2015). It has been previously speculated (Ao et al., 2012; Ganeshan and Wu, 2015; Chang et al., 2022) that there is an inverse relationship between water vapor amount and RO penetration depth, with increased lower atmospheric penetration typically observed in regions away from the tropics, specifically over the dry north pole. The minimum penetration depth from Spire is more spatially homogeneous compared to the other two data sets, showing less sensitivity to surface properties and meteorology.

195

200



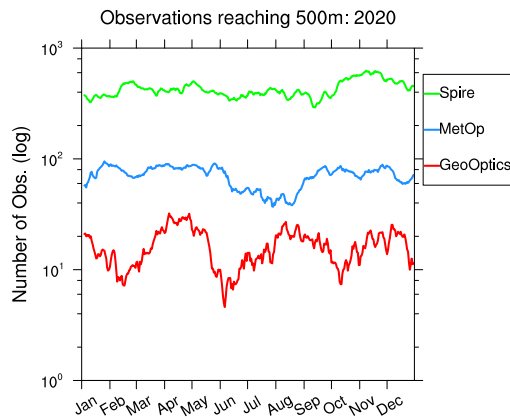
205

Fig. 3 RO penetration statistics over the Arctic Ocean for December 2020 comparing GeoOptics, Spire and MetOp datasets showing **(top)** the minimum altitude of RO penetration and **(bottom)** the RO penetration probability at 500 m altitude.

Based on previous studies involving RO-derived PBLH (Ao et al. 2012; Ganeshan and Wu, 2015), a 500 m cut-off altitude is chosen to select profiles used for retrieving the PBLH. Figure 3 (bottom row) compares the RO penetration probability at 500 m altitude between the three datasets. In general, both commercial products have a high fraction of RO observations (~80%) reaching 500 meters altitude compared to MetOp (~60%).

Figure 4 compares the time-series of total number of available RO observations at 500 m altitude over the Arctic Ocean. Spire has the maximum number of daily observations, nearly an order (two orders) of magnitude greater than MetOp (GeoOptics). We note a reduction of MetOp RO profiles in summer months which are indicative of more stringent quality control criteria, and a similar drop in GeoOptics RO profiles in February, June, and October.

215



220 **Fig. 4** Annual time-series of number of RO observations reaching 500 m altitude or lower over the Arctic Ocean for the year 2020. The daily observations are smoothed using a 5-day running average filter.

3.3 Performance of commercial GNSS RO datasets for refractivity-based PBLH over Arctic

This section will focus on exploring the potential for using commercial RO data for Arctic winter PBL studies using the cut-off altitude threshold of 500 m to select RO profiles, as described previously (section 2.1.3 and section 3.1). Ganeshan and Wu
 225 (2015) showed that the minimum refractivity gradient method works well to detect PBL temperature inversions over the Arctic Ocean during winter months (November – April). Due to the lack of moisture in the atmosphere, the refractivity gradient minimum is found to be sensitive to the positive temperature gradient maxima (i.e. temperature inversions).

Figures 5-7 compare the monthly RO-derived PBLH characteristics for each product during the cold season months of the year
 230 2020 (January – April, and November – December). The adopted methodology (Ganeshan and Wu, 2015) described in section 2.1.3, appears to work well for GeoOptics and MetOp, which clearly show the expected distribution of shallow PBLH over sea ice versus deeper PBLH over the Atlantic sector (based on monthly sea ice distributions shown in Figure 8), with GeoOptics showing a stronger contrast between the two regions. The extreme high values of GeoOptics PBLH estimates in the Atlantic Sector seems to be related to the high minimum penetration altitude in this region (seen in top row of Fig. 3). A seasonal evolution in the retrieved PBLH is evident in both GeoOptics and MetOp datasets with the lowest values generally observed during January, February and March, and highest values in November, which is in good agreement with MERRA-2 derived PBLH (Figure 9). On the other hand, Spire derived mean PBLH appears to have lesser spatial and seasonal variation compared to the other two datasets and compared to MERRA-2, which could be because of the increased vertical smoothing applied to their bending angle product (Bowler, 2020) that may limit the effective vertical resolution of refractivity and the range of
 240 refractivity-derived PBLH values.

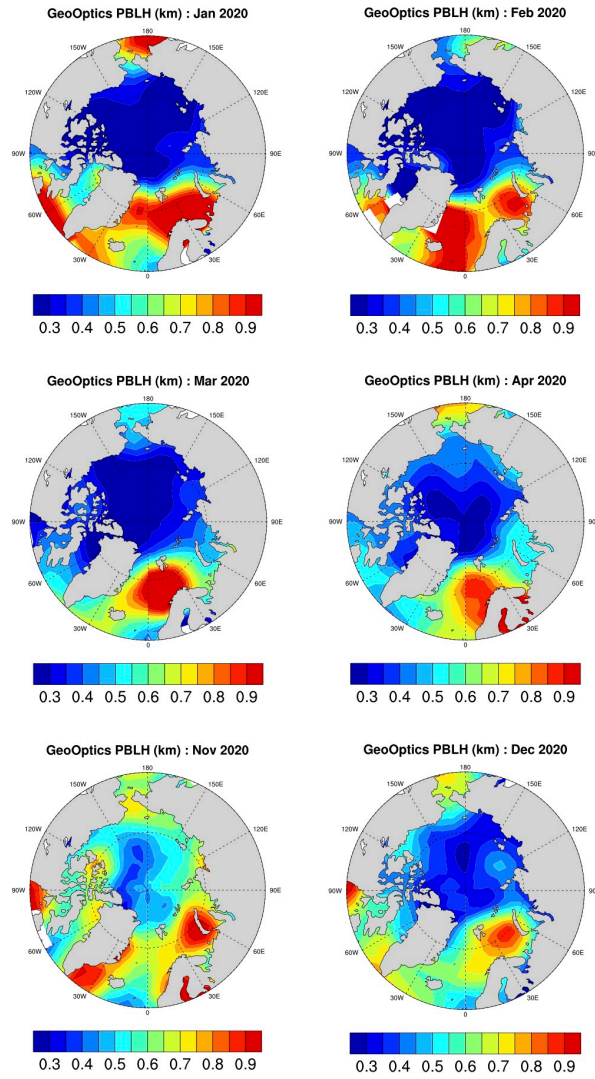
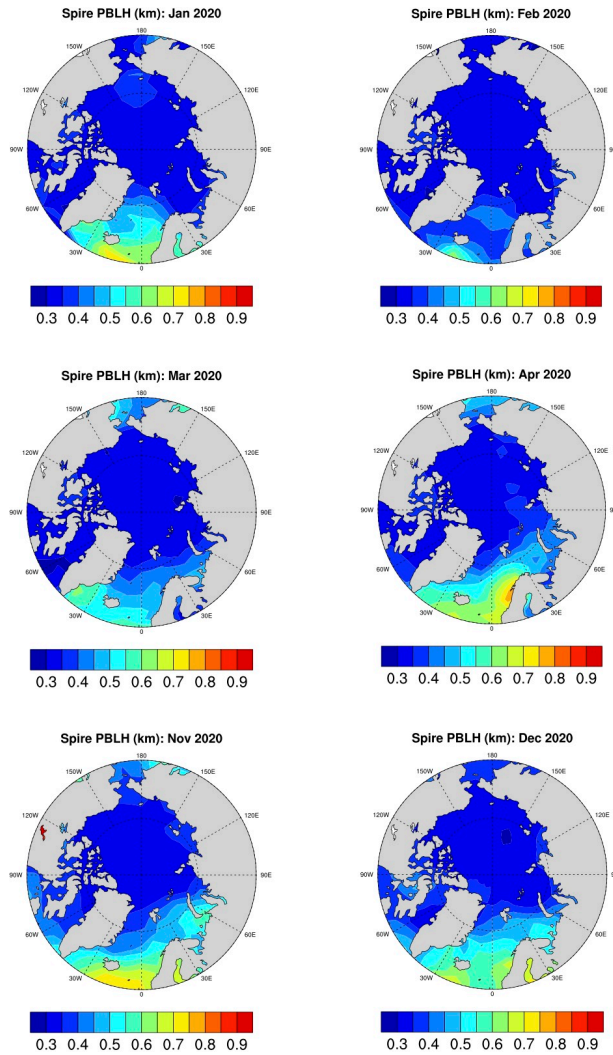
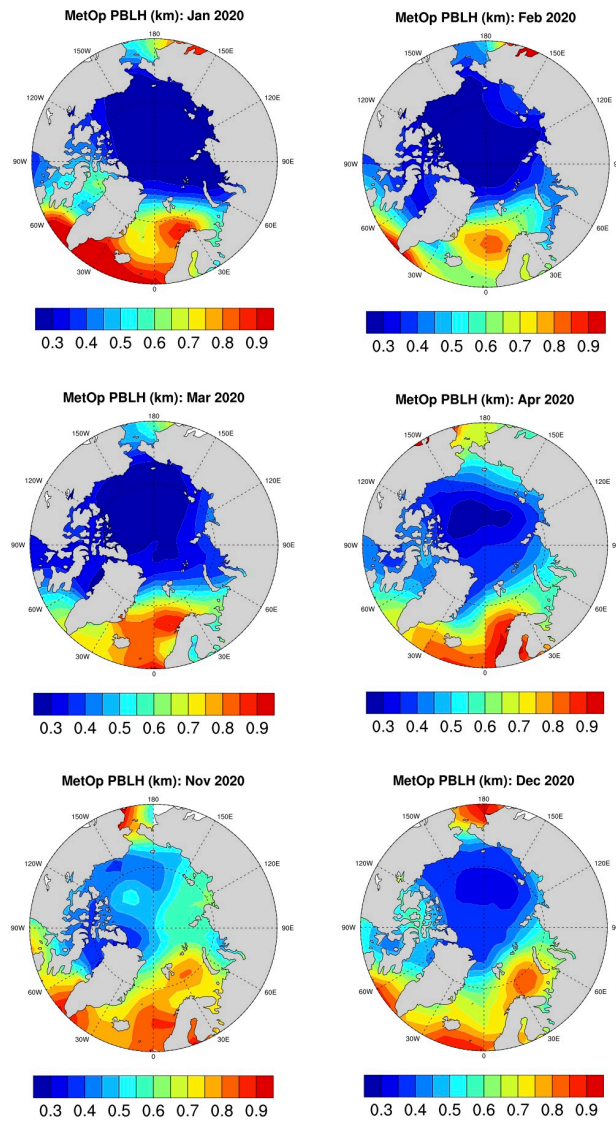


Fig. 5 NASA GeoOptics monthly Arctic PBLH for cold season months of the year 2020.

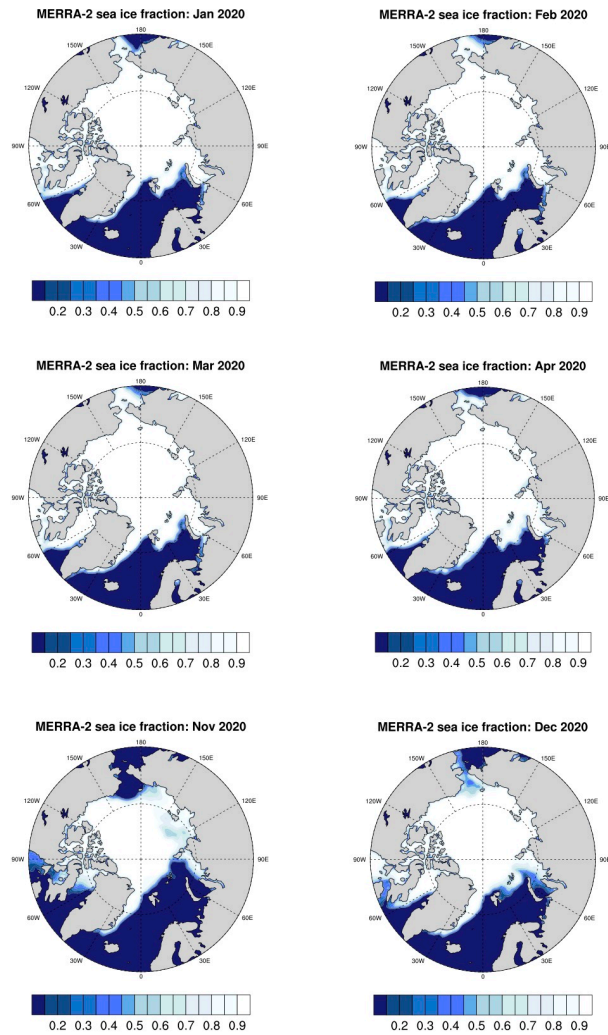


245

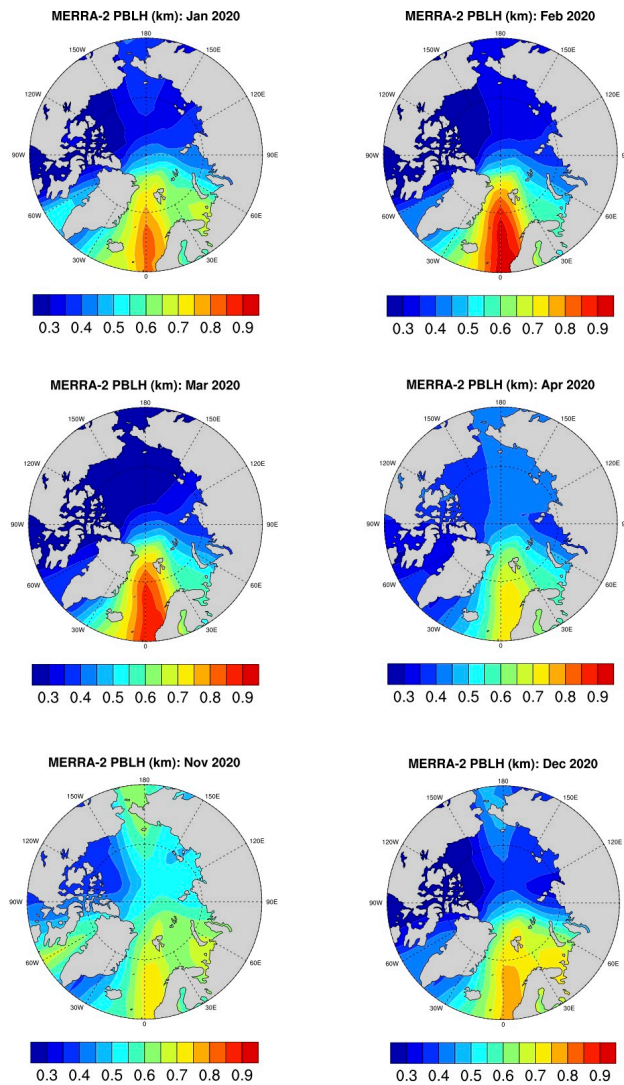
Fig. 6 NASA Spire monthly Arctic PBLH for cold season months of the year 2020.



250 Fig. 7 MetOP monthly Arctic PBLH for cold season months of the year 2020.



255 **Fig. 8** MERRA-2 monthly Arctic sea-ice fraction for cold season months of the year 2020.



260 **Fig. 9** MERRA-2 monthly PBLH showing the seasonal evolution and spatial variability of Arctic PBLH for cold season months of the year 2020.

3.4 Sensitivity to cut-off altitude

As explained in section 1.2, a sampling bias may occur in the retrieved PBLH due to any sharp drop in available RO profiles, thereby necessitating the selection of an optimal cut-off altitude threshold for minimum required RO penetration height. Although the standard cut-off altitude of 500 m has been regarded as sufficient for deriving refractivity-based PBLH from
 265 COSMIC RO observations in the Arctic, it has been noted to be less than ideal for inferring PBL depth in the case of shallow PBLs (Ao et al., 2012) and may even contribute to a positive bias in regions such as the central Arctic Ocean (Ganeshan and Wu, 2015). It appears, however, that the 500 m cut-off altitude when applied to NASA-purchased GeoOptics and MetOp data

is adequate to obtain a realistic representation of the shallow Arctic PBLH. In the case of NASA-purchased Spire data, the derived PBLH values are slightly higher compared to the other two RO datasets and MERRA-2 reanalyses (Fig. 6). It is worth
 270 investigating whether the standard 500 m cut-off altitude is suboptimal for NASA-purchased Spire data.

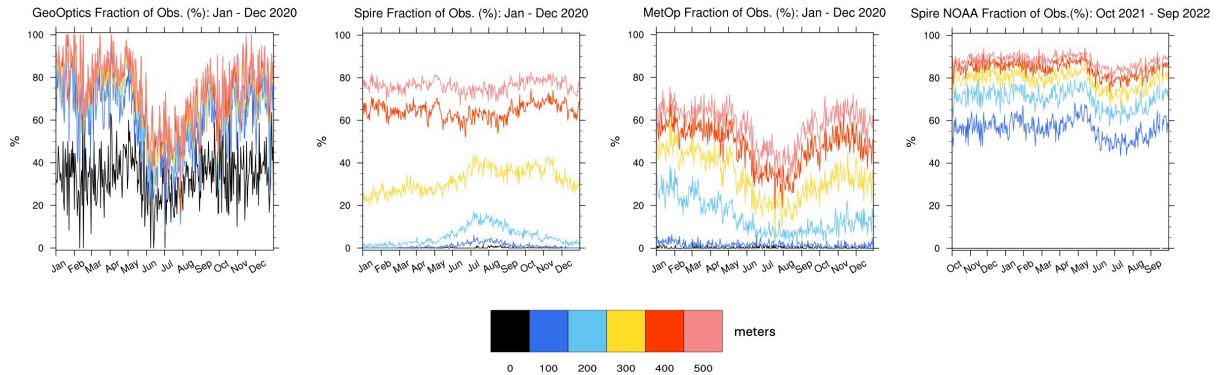


Fig. 10 Annual time-series of penetration probability in the lowest 500 meters for (a) NASA GeoOptics, (b) NASA Spire, (c) MetOp, and (d) NOAA Spire data.

275

Figure 10 shows the annual time-series of the fraction of available RO observations in the lowest 500 m. The percentage of available NASA-purchased Spire RO profiles has two significant drops going from 400 to 300 m and then from 300 to 200 m, which could potentially lead to a positive bias in the retrieved PBLH values when the standard cut-off altitude of 500 m is chosen. No such sharp drop is seen for GeoOptics and MetOp datasets. Moreover, a similar comparison with the Spire NOAA
 280 product shows that this sharp rate of decline only exists in the NASA-purchased Spire data.

Consequently, the PBLH retrievals from NASA Spire are recomputed using a lower cut-off altitude threshold of 300 m, and the resulting PBLH values are found to be significantly lower. Despite an improvement in the PBLH magnitude, the poor granularity in its spatial features and the lack of seasonal variability (as seen in Fig. 6) continue to persist. Figure 11 shows the Arctic PBLH for February 2020 comparing two sets of retrievals from NASA-purchased Spire data using both cut-off altitude thresholds (i.e. 500 m and 300 m). Even though the 300 m cut-off altitude better captures the shallow PBLs, it does not improve the qualitative representation of the Arctic PBLH. On the other hand, comparisons of RO-derived PBLH with NOAA-purchased Spire data showed better agreement with other products (now shown). In summary, an optimal cut-off altitude threshold for NASA Spire data appears to be 300 m, however, the representation of spatiotemporal variability in the derived PBLH remains unsatisfactory. It appears that while RO penetration capability can affect the choice of cut-off altitude and derived PBLH values, the qualitative differences in Arctic PBLH representation are mostly due to different processing
 290 software versions.

Note that, unlike other datasets that show a drop in RO penetration probability over the summer months, NASA-purchased Spire data appears to have no such reduction, signifying less sensitivity to water vapor compared to other missions and UCAR-processed Spire data.

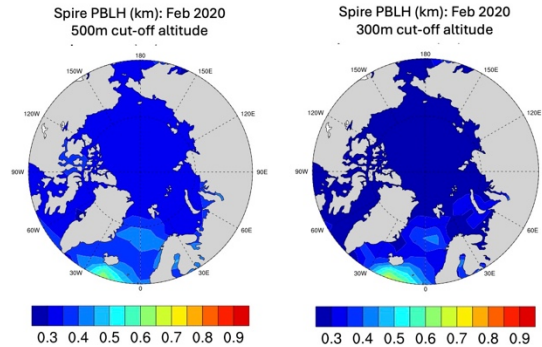


Fig. 11 PBLH retrieved from NASA Spire data using (a) 500 m and (b) 300 m cut-off altitude threshold for minimum RO penetration depth.

4 Summary and Conclusions

300 This study explores the use of commercial GNSS RO neutral atmosphere products from Spire and GeoOptics to advance Arctic PBL studies. The launch of commercial GNSS RO CubeSat receivers, such as Spire and GeoOptics, presents an unparalleled opportunity for high-latitude PBL studies that are presently impacted by the loss of COSMIC-1 and the limited coverage by its successor COSMIC-2. To continue to support PBL studies in polar regions, new GNSS RO products must have sufficient lower atmospheric penetration capability, and the ability to sample shallow PBL temperature inversions that often persist in
 305 polar regions. This study attempts to provide a comparison of the penetration capability of the new commercial and other existing GNSS RO data products in the Arctic as the first step towards establishing a climate-ready, long-term continuous, dataset that can be used for Arctic PBL investigations.

Both commercial products, purchased by NASA, are found to have an improved lower atmospheric penetration capability over the Arctic Ocean compared to contemporaneous MetOp observations from EUMETSAT as evidenced by lower
 310 minimum penetration depths achieved over the frozen Arctic Ocean and higher penetration probability at the standard cut-off altitude of 500 m. We identified that, on average, 80% of GeoOptics RO and Spire RO measurements could probe the troposphere as low as 500 m, as compared to 60% MetOp observations that can measure PBL properties as low as 500 m. The resulting PBLH derived from the commercial RO products, however, seems relatively independent of this advancement. Overall, the monthly mean PBLH pattern and seasonal evolution over the Arctic Ocean are best represented by NASA
 315 GeoOptics and MetOp data, in agreement with MERRA-2. On the other hand, PBLH retrieved from NASA Spire data, despite having improved lower tropospheric penetration, has insufficient spatial granularity and seasonality which is better represented in other datasets.

In fact, the rate of decline of RO penetration within the PBL appears to be an influential factor affecting the choice of the minimum required RO penetration altitude (cut-off altitude) for PBLH retrieval. For products in which the rate of decline

320 is smooth, the standard cut-off altitude for RO penetration depth (i.e. 500 m) works well, however, for products such as NASA
Spire, where the rate of decline is drastic within the lowest 500 meters, the PBLH representation is improved when a lower
cut-off altitude (i.e. 300 m) is used. Regardless, the spatiotemporal variability and qualitative representation of the Arctic
PBLH appears to be independent of the choice of cut-off altitude threshold. A preliminary comparison with NOAA Spire data
325 angle profiles. The methodology used to obtain neutral atmosphere products from excess phase data is thus crucial for both
lower tropospheric penetration probability and for Arctic PBLH representation.

Acknowledgments: This research was done in collaboration with Jet Propulsion Laboratory, California Institute of
Technology under a contract with the National Aeronautics and Space Administration (80NM0018D0004) in addition to
330 support from NASA grant 80NSSC23K0385. The research described in this paper was partially carried out at the Jet Propulsion
Laboratory, California Institute of Technology, under a contract with the National Aeronautics and Space Administration.

Competing Interests: The contact author has declared that none of the authors has any competing interests.

335 **References**

- Ao, C. O., D. E. Waliser, S. K. Chan, J.-L. Li, B. Tian, F. Xie, and A. J. Mannucci (2012), Planetary boundary layer heights
from GPS radio occultation refractivity and humidity profiles, *J. Geophys. Res.*, 117, D16117, doi:10.1029/2012JD017598
- 340 Basha, G. and M.V. Ratnam (2009), Identification of atmospheric boundary layer height over a tropical station using high-
resolution radiosonde refractivity profiles: Comparison with GPS radio occultation measurements, *Journal of Geophysical
Research*, 114, <https://doi.org/10.1029/2008jd011692>.
- Chang, H., J. Lee, H. Yoon, Y. J. Morton, and A. Saltman, 2022: Performance assessment of radio occultation data from
345 GeoOptics by comparing with COSMIC data. *Earth, Planets
and Space*, 74, 108.
- Ding, F., L. Iredell, M. Theobald, J. Wei, and D. Meyer (2021), PBL Height From AIRS, GPS RO, and MERRA-2 Products
in NASA GES DISC and Their 10-Year Seasonal Mean Intercomparison, *Earth and Space Science*, 8, e2021EA001859,
350 <https://doi.org/10.1029/2021EA001859>.
- E. Bowler, N. (2020). An assessment of GNSS radio occultation data produced by Spire. *Quarterly Journal of the Royal
Meteorological Society*, 146(733), 3772-3788.

- 355 Ganeshan, M., & Wu, D. L. (2015). An investigation of the Arctic inversion using COSMIC RO observations. *Journal of Geophysical Research: Atmospheres*, 120(18), 9338-9351.
- Ganeshan, M., & Yang, Y. (2019). Evaluation of the Antarctic boundary layer thermodynamic structure in MERRA2 using dropsonde observations from the Concordiasi campaign. *Earth and Space Science*, 6(12), 2397-2409.
- 360
- Gelaro, R., McCarty, W., Suárez, M. J., Todling, R., Molod, A., Takacs, L., ... & Zhao, B. (2017). The modern-era retrospective analysis for research and applications, version 2 (MERRA-2). *Journal of climate*, 30(14), 5419-5454.
- Guo, P., Y.-H. Kuo, S. V. Sokolovskiy, and D. H. Lenschow (2011), Estimating atmospheric boundary layer depth using
365 COSMIC radio occultation data, *J. Atmos. Sci.*, 68, 1703–1713, doi:10.1175/2011JAS3612.1.
- Jarraud, M.: Guide to meteorological instruments and methods of observation (WMO-No. 8). *World Meteorological Organisation: Geneva, Switzerland*, 29.
- 370 Jensen, A. S., Lohmann, M. S., Nielsen, A. S., and Benzon, H.-H. (2004). Geometrical optics phase matching of radio occultation signals, *Radio Science*, 39, n/a-n/a, <https://doi.org/10.1029/2003rs002899>.
- Kalmus, P., Ao, C. O., Wang, K.-N., Manzi, M. P., and Teixeira, J. (2022). A high-resolution planetary boundary layer height seasonal climatology from GNSS radio occultations, *Remote Sensing of Environment*, 276, 113037,
375 <https://doi.org/10.1016/j.rse.2022.113037>.
- Lock, A. P., Brown, A. R., Bush, M. R., Martin, G. M., & Smith, R. N. B. (2000). A new boundary layer mixing scheme. Part I: Scheme description and single-column model tests. *Monthly Weather Review*, 138, 3187–3199.
- 380 Louis, J. F. (1982). A short history of the operational PBL parameterization at ECMWF. In *Workshop on Planetary Boundary Layer Parameterization, ECMWF, England, 1982*.
- Maturilli, M., Holdridge, D. J., Dahlke, S., Graeser, J., Sommerfeld, A., Jaiser, R., Deckelmann, H., Schulz, A.: Initial radiosonde data from 2019-10 to 2020-09 during project MOSAiC. *Alfred Wegener Institute, Helmholtz Centre for Polar and
385 Marine Research, Bremerhaven, PANGAEA*, <https://doi.org/10.1594/PANGAEA.928656>, 2021

Männel, B., Zus, F., Dick, G., Glaser, S., Semmling, M., Balidakis, K., ... & Schuh, H.: GNSS-based water vapor estimation and validation during the MOSAiC expedition. *Atmospheric Measurement Techniques*, 14(7), 5127-5138, 2021.

390 McGrath-Spangler, E. L., Molod, A., Ott, L. E., & Pawson, S. (2015). Impact of planetary boundary layer turbulence on model climate and tracer transport. *Atmospheric Chemistry and Physics*, 15(13), 7269-7286.

National Academies of Sciences, Engineering, and Medicine. (2018). *Thriving on our changing planet: A decadal strategy for earth observation from Space*. The National Academies Press. <https://doi.org/10.17226/24938>

395

Nelson, K. J., Xie, F., Ao, C. O., and Oyola-Merced, M. I. (2021). Diurnal Variation of the Planetary Boundary Layer Height Observed from GNSS Radio Occultation and Radiosonde Soundings over the Southern Great Plains, *Journal of Atmospheric and Oceanic Technology*, 38, 2081–2093, <https://doi.org/10.1175/jtech-d-20-0196.1>.

400 Qiu, C., Wang, X., Li, H., Zhou, K., Zhang, J., Li, Z., Liu, D., and Yuan, H. (2023). A Comparison of Atmospheric Boundary Layer Height Determination Methods Using GNSS Radio Occultation Data, *Atmosphere*, 14, 1654, <https://doi.org/10.3390/atmos14111654>.

ROM SAF (2019): ROM SAF Radio Occultation Interim Climate Data Record - Metop, EUMETSAT SAF on Radio
405 Occultation Meteorology, DOI: 10.15770/EUM_SAF_GRM_0006. http://doi.org/10.15770/EUM_SAF_GRM_0006

Seidel, D. J., Ao, C. O., and Li, K. (2010). Estimating climatological planetary boundary layer heights from radiosonde observations: Comparison of methods and uncertainty analysis, *Journal of Geophysical Research*, 115, <https://doi.org/10.1029/2009jd013680>.

410

Seidel, D. J., Zhang, Y., Beljaars, A., Golaz, J.-C., Jacobson, A. R., and Medeiros, B. (2012). Climatology of the planetary boundary layer over the continental United States and Europe, *Journal of Geophysical Research: Atmospheres*, 117, n/a-n/a, <https://doi.org/10.1029/2012jd018143>.

415 Teixeira, J., Piepmeier, J., Nehrir, A., Ao, C., Chen, S., Clayson, C. A., et al. (2021). NASA planetary boundary layer (PBL) incubation study.

UCAR, “FORMOSAT-3/COSMIC-1 2021 Reprocessing Data Release”, Nov 29 2022, FORMOSAT-3/COSMIC-1 2021
Reprocessing Data, https://data.cosmic.ucar.edu/gnss-ro/cosmic1/repro2021/UCAR_COSMIC1_2021_Repro_Notes.pdf.

420 Access Date: 04/29/2024.

Winning, T. E., Chen, Y.-L., and Xie, F., (2017). Estimation of the marine boundary layer height over the central North Pacific using GPS radio occultation, *Atmospheric Research*, 183, 362–370, <https://doi.org/10.1016/j.atmosres.2016.08.005>

425 Wu, D. L., Gong, J., & Ganeshan, M. (2022). GNSS-RO Deep Refraction Signals from Moist Marine Atmospheric Boundary Layer (MABL). *Atmosphere*, 13(6), 953.